Supplementary Information

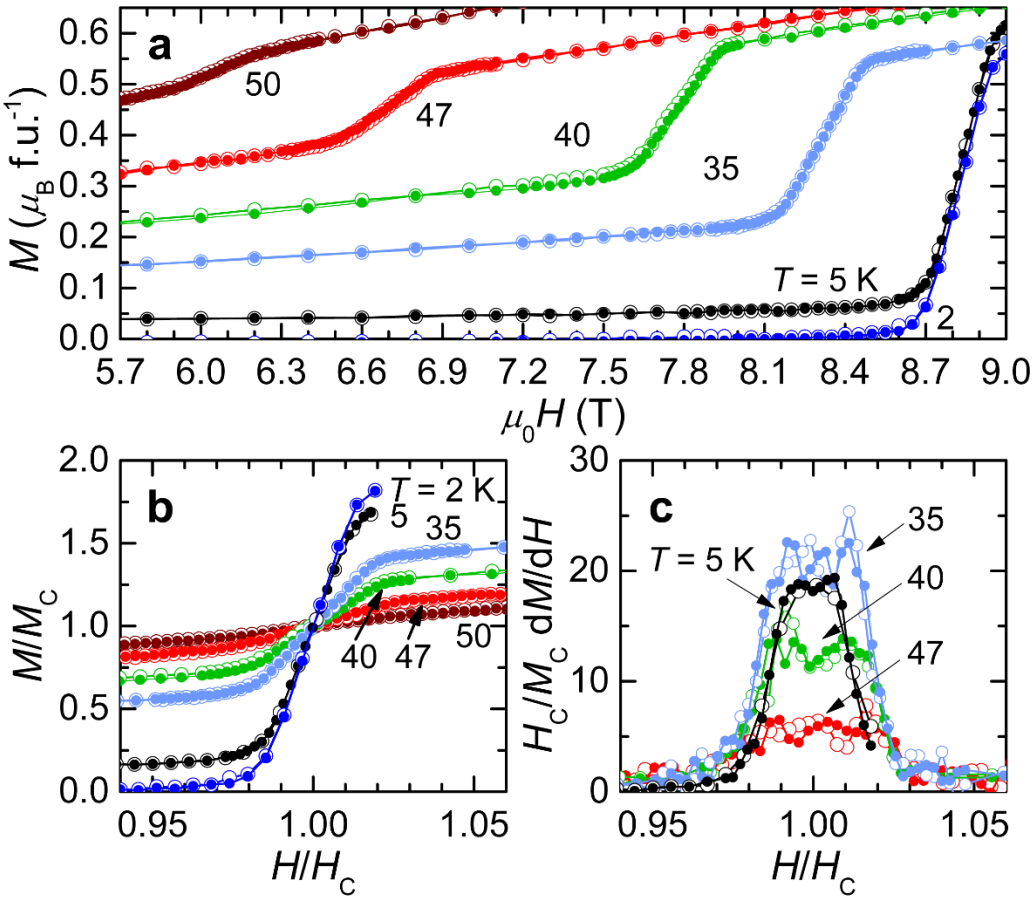

Supplementary Figure 1 | Magnetic field dependence of magnetization.

The details of magnetic field dependence of isothermal magnetization ($M(H)$) have been investigated with magnetic fields stabilized at each field strength to explore the hysteric characteristics of the spin-flop transition in Ni_3TeO_6. (a) depicts $M(H)$ of a Ni_3TeO_6 single crystal in a narrow magnetic field range around the critical magnetic field (H_c) at T = 50, 47, 45, 40, 35, 5, and 2 K. Magnetic field was applied along the c-axis. Closed (open) circles depict ramping-up (ramping-down) data. Within the error bar of ±10 Oe, no hysteresis across H_c is observed. (b) shows M/M_c as a function of H/H_c, in which M and H are normalized by H_c and $M_c = M_{H=Hc}$, respectively. At T = 50, 47, 40, 35, 5, and 2 K, H_c's are 6.0552, 6.6905, 7.7682, 8.3077, 8.8413, and 8.8298 T and the corresponding M_c's are 0.5270, 0.4516, 0.4501, 0.3874, 0.3652, and 0.3078 μ_B f.u.$^{-1}$, respectively. (c) Magnetic field derivative of normalized magnetization (d[M/M_c]/d[H/H_c]) vs. H/H_c at T = 47, 40, 35, and 5 K. The presence of two peaks, evident particularly at low temperatures, in the derivative are consistent with the existence of an intermediate sate, which is similar with the intermediate monoclinic phase between two structural phases in ferroelectrics.

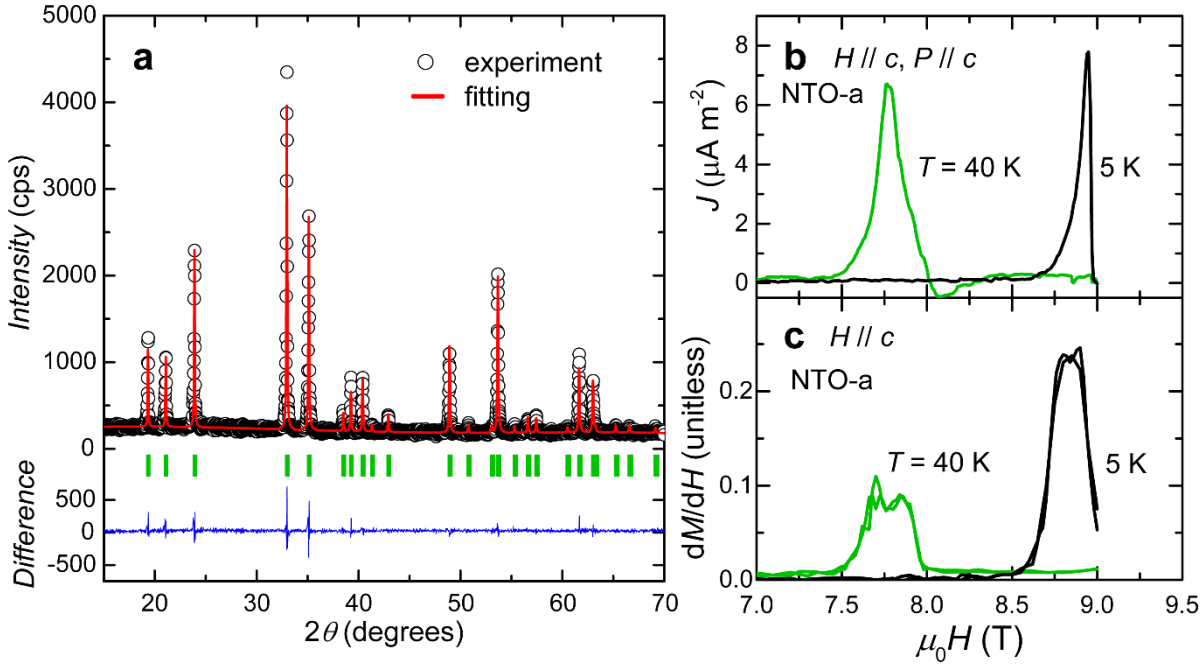

Supplementary Figure 2 | Structure refinement and magnetic field dependence of magnetization and polarization of NTO-a.

Powder x-ray diffraction experiment and Rietveld refinement have been performed on crushed powders of a Ni_3TeO_6 single crystal. (a) Observed, calculated, and difference x-ray powder diffraction patterns for a Ni_3TeO_6 single crystal at room temperature are represented. Atomic parameters in the refinement is summarized in supplementary Table S1. (b) and (c) compare the magnetic field dependence of magnetoelectric current $J(H)$ and magnetic field derivative of magnetization, dM/dH, of NTO-a (an as-grown Ni_3TeO_6 single crystal) at 40 K and 5 K. Associated with a spin-flop transition, both $J(H)$ and dM/dH exhibit sharp peak features at the same critical magnetic field, which depends on temperature.

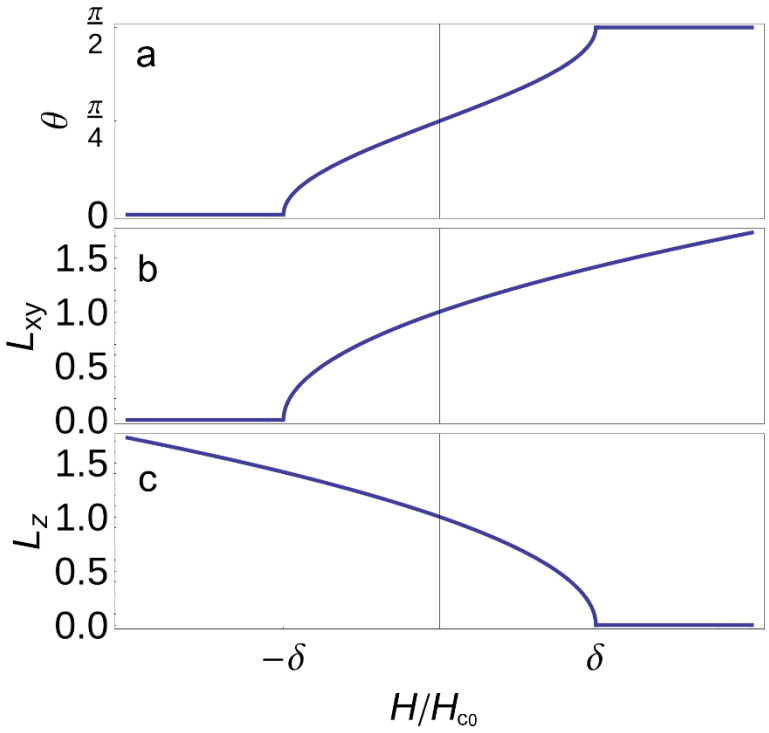

Supplementary Figure 3 | Rotation of the antiferromagnetic order parameter for $K_4 < 0$.
For $K_4 < 0$, the minimum of free energy continuously moves from $\theta = 0$ to $\theta = \pi/2$ as magnetic field increases. Plotted is the corresponding evolution of (a) the direction of antiferromagnetic order parameter and the amplitudes of its (b) *ab*-axis and (c) *c*-plane components. For $K_4 < 0$, with the increase of magnetic field along the *c* axis the system goes from low magnetic field state $\vec{\mathbf{L}} \parallel \mathbf{c}$ to the spin-flopped state $\vec{\mathbf{L}} \perp \mathbf{c}$ through an intermediate state, in which the AFM order parameter continuously rotates between these limiting positions. The apparent second-order behavior at $+\delta$ is broadened into a continuous transition over a small range of *H* if higher-order terms are taken into account. Within our simplified Landau theory the angle $\boldsymbol{\theta}$, describing the rotation angle, changes with the applied magnetic field as shown in Figure S3. We assume that the AFM order parameter has the form of $\vec{\mathbf{L}} = (\boldsymbol{L}\sin\boldsymbol{\theta}, \mathbf{0}, \boldsymbol{L}\cos\boldsymbol{\theta})$. Thus, it rotates in the *ac*-plane in our model. In general, $\vec{\mathbf{L}} = (\boldsymbol{L}\sin\boldsymbol{\theta}\cos\boldsymbol{\phi}, \boldsymbol{L}\sin\boldsymbol{\theta}\sin\boldsymbol{\phi}, \boldsymbol{L}\cos\boldsymbol{\theta})$, where $\boldsymbol{\phi}$ is an azimuthal angle, and the leading *ab*-plane anisotropy term is proportional to $\boldsymbol{f_{ab}} \sim \boldsymbol{L^6}\cos 6\boldsymbol{\phi}$, which leads to six different free energy minima, differing by $\pi/3$.

Atom	x	y	z
Te	1/3	2/3	0.3824
Ni1	1/3	2/3	0.1715
Ni2	1	1	0.2124
Ni3	2/3	1/3	0.3559
O1	0.6333	0.6664	0.2846
O2	0.9879	0.6222	0.4398

Supplementary Table 1 | Atomic parameters from Rietveld refinement.